Pergamon

PII: S0045-7949(96)00062-4

Computers & Structures Vol. 61, No. 3, pp. 529–538, 1996
Published by Elsevier Science Ltd
Printed in Great Britain
0045-7949/96 $15.00 + 0.00

AN EXPLICIT PLANE QUADRILATERAL ELEMENT FOR NONLINEAR MATERIAL ANALYSIS

E. Saether

U.S. Army Research Laboratory, Aberdeen Proving Ground, Materials Directorate—Chestnut Run
Attn: AMSEL-MA-C, Aberdeen, MD 21805, U.S.A.

(*Received* 16 *March* 1995)

Abstract—A general methodology for deriving explicit element stiffness matrices in hybrid stress formulations is extended to incorporate nonconstant material properties over the element domain for nonlinear elastic analysis. The technique utilizes special stress field transformations to simplify the stiffness definition together with an assumed variation of material properties using isoparametric interpolation functions. The developed technique eliminates the need for numerical integration and matrix inversions, resulting in a substantial increase in computation efficiency. The methodology is demonstrated with the Pian–Sumihara plane quadrilateral element. Published by Elsevier Science Ltd

INTRODUCTION

The study of hybrid–mixed element formulations has generated much research into minimizing the computational cost to make such elements competitive with displacement-based elements. In hybrid formulations, many insightful treatments have been utilized to reduce computations, the most notable have been simplifying approximations made to the flexibility or complementary energy matrix inherent to the technique [1–3]. The hybrid stress method has many desirable features which, aside from superior performance over similar displacement-based elements, include the inherent expressibility of most hybrid element constituent matrices in algebraic form. This feature is due to the absence of the inverse Jacobian determinant in the stiffness definition which, in displacement-based continuum elements under general distortion, result in integrands involving rational functions which are only approximated through numerical quadrature. A method has recently been developed by the author for simplifying the definition of hybrid element stiffness matrices through special transformations of assumed stress fields [4, 5]. These transformations effect the removal of the complementary energy matrix, thus permitting an explicit evaluation of stiffness coefficients to be accomplished. The resulting algebraic expressions allow the generation of element stiffness matrices requiring a fraction of the computational cost of a numerical evaluation. Of interest is the extension to nonlinear elastic problems which, within the framework of finite element solution methods, usually require computationally intensive, incremental or iterative solution procedures. To reduce the cost of reforming global stiffnesses during update in, for example, a full or modified Newton–Raphson procedure, the current study aims to incorporate nonconstant material properties in the method of Ref. [4]. As an initial effort, an explicit formulation will be derived for the four-node Pian–Sumihara hybrid quadrilateral element [6].

VARIATIONAL BASIS

As detailed in Ref. [6], the Hellinger–Reissner functional is utilized to define the structure of the element matrices. This functional is given by

$$\Pi_R = \int_v [(-1/2)\sigma^T \mathbf{S}\sigma + \sigma^T(Lu)]\, dv, \qquad (1)$$

where σ is the assumed stress field, $\mathbf{S}$ is the material compliance matrix, u is the assumed displacement fields and L is the differential operator relating strains to displacements.

The assumed stresses are represented by

$$\sigma = \mathbf{P}\boldsymbol{\beta}, \qquad (2)$$

where $\mathbf{P}$ is a matrix of polynomial terms and $\boldsymbol{\beta}$ is a vector of undetermined expansion coefficients. Incompatible displacement fields are introduced such that the displacement field is assumed over the element domain as

$$u = u_q + u_i = Nq + M\lambda, \qquad (3)$$

where N and M are compatible and incompatible displacement shape functions, respectively, q are nodal displacements and λ are Lagrange multipliers which enforce internal constraints. The resulting energy functional is given by

$$\Pi_R = \int_v [(-1/2)\sigma^T \mathbf{S}\sigma + \sigma^T(Lu_q) - (L^T\sigma)^T u_\lambda]\, dv. \tag{4}$$

In the form of eqn (4), the incompatible displacements act to variationally enforce the field equilibrium conditions. These variational constraints are applied *a priori* to the assumed stress modes which condense the influence of the incompatible modes into the element formulation.

Substituting eqns (2) and (3) into eqn (4) and taking variations with respect to β and q result in an expression for the element stiffness matrix given by

$$\mathbf{K} = \mathbf{G}^T\mathbf{H}^{-1}\mathbf{G}, \tag{5}$$

where

$$\mathbf{H} = \int_v \mathbf{P}^T\mathbf{S}\mathbf{P}\, dv, \tag{6}$$

$$\mathbf{G} = \int_v \mathbf{P}^T\mathbf{B}\, dv, \tag{7}$$

and $\mathbf{B}$ is the strain-displacement matrix. In the above formulation, the *a priori* condensation of the incompatible displacement modes results in an $\mathbf{H}$ matrix which is fully populated and has hitherto required the inversion of a full matrix of order $\dim(\beta)$.

NONLINEAR ELEMENT STIFFNESS DEFINITION

The procedure developed in Ref. [4] for simplifying eqn (5) is extended to account for nonconstant material properties. The method utilizes a sequence of permissible transformations of assumed stress fields to simplify the stiffness definition, together with an assumed order of interpolation of material properties over the element domain. The assumed stresses are first transformed using a symmetric matrix denoted by $\mathbf{D}$ and introduced as

$$\mathbf{P} = \mathbf{I}\mathbf{P} = (\mathbf{D}\mathbf{D}^{-1})\mathbf{P} = \mathbf{D}(\mathbf{D}^{-1}\mathbf{P}) = \mathbf{D}\bar{\mathbf{P}}, \tag{8}$$

where the $\mathbf{D}$ matrix is defined as

$$\mathbf{D} = \mathbf{S}^{-1/2}. \tag{9}$$

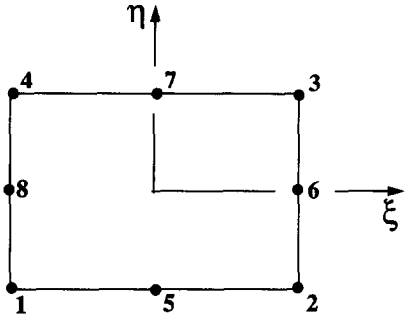

Fig. 1. Evaluation points used for material interpolation.

The inverse square root of the compliance matrix is obtained through a standard spectral decomposition [7] using the material stiffness matrix, $\mathbf{C}$, given by

$$\mathbf{S}^{-1/2} = \mathbf{C}^{1/2} = \mathbf{Q}\Lambda^{1/2}\mathbf{Q}^T, \tag{10}$$

where $\mathbf{Q}$ is a unitary matrix composed of normalized system eigenvectors and Λ is a diagonal matrix of associated eigenvalues. Explicit expressions for Λ and $\mathbf{Q}$ for an orthotropic material are presented in Appendix I.

The extension to nonconstant material properties requires that the compliance matrix be interpolated over the element domain. For the quadrilateral plane element under study a bilinear isoparametric field is sufficient for interpolating compliance properties; however, the derived $\mathbf{D}$ matrix is a nonlinear function of $\mathbf{S}$ thus requiring a higher order interpolation. A quadratic isoparametric field is adopted in which the material matrices are computed at the stress recovery or material evolution points depicted in Fig. 1. Thus, at arbitrary points over the element domain $\mathbf{D} = \bar{\mathbf{S}}^{-1/2}$ and the interpolation results in the relationship $\bar{\mathbf{S}} = \mathbf{S}$ being strictly valid at the recovery points and approximate elsewhere. The accuracy of this approximation is discussed later in Remark I. The interpolation is given by

$$\Omega(\xi, \eta) = \sum_{i=1}^{8} N_i(\xi,\eta)\Omega_i, \tag{11}$$

where Ω_i represents the material $\mathbf{D}$ and $\mathbf{D}^{-1}$ matrices computed at the ith stress recovery point and N_i are the associated quadratic-order isoparametric shape functions. Interpolation of the material matrices over the element domain may be expressed as

$$\Omega(\xi, \eta) = A_1 + A_2\xi + A_3\eta + A_4\xi^2 + A_5\eta^2 + A_6\xi\eta + A_7\xi^2\eta + A_8\xi\eta^2, \tag{12}$$

where the constant matrices, A_i, are given by

$$\begin{Bmatrix} A_1 \\ A_2 \\ A_3 \\ A_4 \\ A_5 \\ A_6 \\ A_7 \\ A_8 \end{Bmatrix} = \frac{1}{4} \begin{bmatrix} -1 & -1 & -1 & -1 & 2 & 2 & 2 & 2 \\ & & & & & 2 & & -2 \\ & & & & -2 & & 2 & \\ 1 & -1 & 1 & -1 & & & & \\ 1 & 1 & 1 & 1 & -2 & & -2 & \\ -1 & -1 & 1 & 1 & & 2 & & -2 \\ -1 & -1 & 1 & 1 & 2 & & -2 & \\ -1 & 1 & 1 & -1 & & -2 & & 2 \end{bmatrix} \begin{Bmatrix} \Omega_1 \\ \Omega_2 \\ \Omega_3 \\ \Omega_4 \\ \Omega_5 \\ \Omega_6 \\ \Omega_7 \\ \Omega_8 \end{Bmatrix} \tag{13}$$

Substitution of eqn (8) into eqn (6) yields the flexibility matrix as

$$\mathbf{H} = \int_{-1}^{1} \int_{-1}^{1} [|\mathbf{J}| \bar{\mathbf{P}}^{\mathrm{T}} \mathbf{D}^{\mathrm{T}} \mathbf{S} \mathbf{D} \bar{\mathbf{P}}] \, \mathrm{d}\xi \, \mathrm{d}\eta, \tag{14}$$

where, from the definition of **D** and the symmetry of both **S** and **D** we obtain

$$\mathbf{D}^{\mathrm{T}} \mathbf{S} \mathbf{D} = \bar{\mathbf{S}}^{-1/2} \mathbf{S} \bar{\mathbf{S}}^{-1/2} = \mathbf{S} \bar{\mathbf{S}}^{-1} \approx \mathbf{I}. \tag{15}$$

The approximation rapidly approaches an identity as the interpolation order of **D** increases and as the variation of material properties over the element diminishes. The flexibility matrix is thereby closely approximated by

$$\mathbf{H} \approx \int_{-1}^{1} \int_{-1}^{1} [|\mathbf{J}| \bar{\mathbf{P}}^{\mathrm{T}} \bar{\mathbf{P}}] \, \mathrm{d}\xi \, \mathrm{d}\eta. \tag{16}$$

A second field transformation uses eqn (16) to define a weighted inner product for use in a Gram–Schmidt procedure to generate an orthonormal spanning set of stress modes, $\mathbf{P}^*$. This modal set is formed as a special linear combination of the modes present in $\bar{\mathbf{P}}$ and constitutes an alternative basis set which spans the original stress space. The weighted inner product is therefore defined as

$$\langle \bar{P}_i, \bar{P}_j \rangle = \int_{-1}^{1} \int_{-1}^{1} [|\mathbf{J}| \bar{P}_i^{\mathrm{T}} P_j] \, \mathrm{d}\xi \, \mathrm{d}\eta \tag{17}$$

The linear combination yielding a sequence of orthogonal stress modes is given by

$$V_i = \begin{cases} \bar{P}_i & i = 1, \\ \bar{P}_i - \sum_{j=1}^{i-1} \langle P_j^*, \bar{P}_i \rangle P_j^* & i > 1, \end{cases} \tag{18}$$

which are normalized to form basis vectors, P_i^*, as

$$P_i^* = \langle V_i, V_i \rangle^{-1/2} V_i. \tag{19}$$

In the definition of $\bar{\mathbf{P}}$, the $\bar{\mathbf{D}}^{-1}$ matrix is interpolated according to eqn (12) and carried into the subsequent orthonormalization of assumed stress modes. For the present study, however, a simplification is adopted wherein the **D** matrix is interpolated according to eqn (12) while its inverse is obtained from an area average obtained by integrating over the element domain. This operation is not required, but is utilized in the present study to simplify the expressions for the orthonormalized stress modes, $\mathbf{P}^*$, while maintaining an adequate approximation for the material properties. The inverse is thus defined as

$$\mathbf{D}^{-1} = \left[\frac{1}{4} \int_{-1}^{1} \int_{-1}^{1} \mathbf{D}(\xi, \eta) \, \mathrm{d}\xi \, \mathrm{d}\eta \right]^{-1}, \tag{20}$$

and the relationship

$$\mathbf{D}(\xi, \eta) \mathbf{D}^{-1} \approx \mathbf{I}, \tag{21}$$

is satisfied in an integral sense for nonconstant material properties and pointwise for constant properties over the element domain. Substitution of $\mathbf{P}^*$ into eqn (16) yields by definition

$$\mathbf{H} = \int_{-1}^{1} \int_{-1}^{1} [|\mathbf{J}| \mathbf{P}^{*\mathrm{T}} \mathbf{P}^*] \, \mathrm{d}\xi \, \mathrm{d}\eta \equiv \mathbf{I}. \tag{22}$$

The new basis for the element stress field is given by

$$\mathbf{P} = \mathbf{D}\mathbf{P}^*, \tag{23}$$

and the expression for the element stiffness matrix reduces to

$$\mathbf{K} = \mathbf{G}^{\mathrm{T}} \mathbf{G}. \tag{24}$$

Separating out the Jacobian determinant from the isoparametric strains as

$$\mathbf{B} = \frac{1}{|\mathbf{J}|} \mathbf{B}^*(\xi, \eta, \zeta), \tag{25}$$

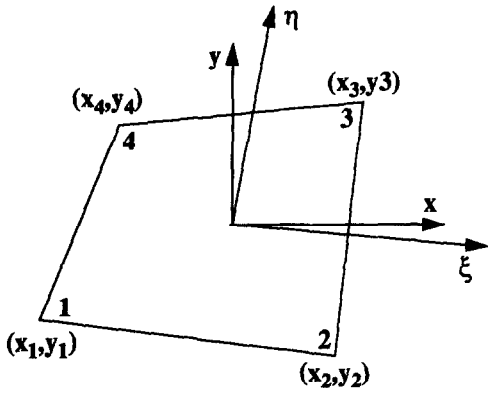

Fig. 2. Quadrilateral element configuration.

and substituting eqns (23) and (25) into eqn (7), the **G** matrix definition becomes

$$\mathbf{G} = \int_{-1}^{1}\int_{-1}^{1} [\mathbf{P}^{*\mathrm{T}}\mathbf{D}\mathbf{B}^{*}]\,\mathrm{d}\xi\,\mathrm{d}\eta. \tag{26}$$

The absence of the Jacobian determinant in the denominator permits a direct derivation of algebraic expressions for the **G** matrix coefficients which incorporate a nonconstant field of material properties over the element domain. The explicit form of the element stiffness matrix is then obtained from eqn (24).

NONLINEAR PIAN–SUMIHARA ELEMENT

The configuration of the Pian–Sumihara element and node numbering are depicted in Fig. 2. The displacement functions u_q are given by

$$\mathbf{u}_q = \begin{pmatrix} u_q \\ v_q \end{pmatrix} = \frac{1}{4}\sum_{i=1}^{4}(1+\xi_i\xi)(1+\eta_i\eta)\begin{pmatrix} u_i \\ v_i \end{pmatrix}. \tag{27}$$

The tensorial stress field is transformed to physical or Cartesian coordinates using Jacobians computed at the element centroid as

$$\sigma^{kl} = (J_0)^k_i\,(J_0)^l_j\,\tau^{ij}. \tag{28}$$

Performing the initial transformation of stresses given by eqn (8) results in the Cartesian stress field given by

$$\sigma = [\sigma_x, \sigma_y, \tau_{xy}]^{\mathrm{T}} = \bar{\mathbf{P}}\boldsymbol{\beta}, \tag{29}$$

where

$$\bar{\mathbf{P}} = \begin{bmatrix} 1 & & & c_{11}\xi & c_{12}\eta \\ & 1 & & c_{21}\xi & c_{22}\eta \\ & & 1 & c_{31}\xi & c_{32}\eta \end{bmatrix}, \tag{30}$$

and the coefficients c_{ij} are obtained from the product of $\mathbf{D}^{-1}$ and a transformation matrix relating tensorial stresses to Cartesian components. This relationship is given by

$$[c_{ij}] = \mathbf{D}^{-1}\boldsymbol{\Gamma} = \begin{bmatrix} \bar{d}_{11} & \bar{d}_{12} & \\ \bar{d}_{21} & \bar{d}_{22} & \\ & & \bar{d}_{33} \end{bmatrix}\begin{bmatrix} a_2^2 & a_1^2 \\ b_2^2 & b_1^2 \\ a_2b_2 & a_2b_1 \end{bmatrix}.$$

The geometric parameters a_i and b_i are obtained from the mapping between physical and natural coordinates given by

$$\begin{aligned} x &= a_0 + a_1\xi + a_2\eta + a_3\xi\eta, \\ y &= b_0 + b_1\xi + b_2\eta + b_3\xi\eta, \end{aligned} \tag{31}$$

where

$$\begin{bmatrix} a_0 & b_0 \\ a_1 & b_1 \\ a_2 & b_2 \\ a_3 & b_3 \end{bmatrix} = \tfrac{1}{4}\begin{bmatrix} 1 & 1 & 1 & 1 \\ -1 & 1 & 1 & -1 \\ -1 & -1 & 1 & 1 \\ 1 & -1 & 1 & -1 \end{bmatrix}\begin{bmatrix} x_1 & y_1 \\ x_2 & y_2 \\ x_3 & y_3 \\ x_4 & y_4 \end{bmatrix}$$

As detailed in Ref. [6], stresses are defined in natural or tensorial coordinates and incompatible displacement modes are introduced to complete the quadratic order of the assumed isoparametric displacement field. These modes are condensed *a priori* into the element formulation through constraint conditions on the assumed stress modes.

The weighted orthonormalized stress modes are obtained as

$$\mathbf{P}^{*} = \begin{bmatrix} p^{*}_{13} & 0 & 0 & p^{*}_{42}\xi + p^{*}_{43} & p^{*}_{51}\eta + p^{*}_{52}\xi + p^{*}_{53} \\ 0 & p^{*}_{26} & 0 & p^{*}_{45}\xi + p^{*}_{46} & p^{*}_{54}\eta + p^{*}_{55}\xi + p^{*}_{56} \\ 0 & 0 & p^{*}_{39} & p^{*}_{48}\xi + p^{*}_{49} & p^{*}_{57}\eta + p^{*}_{58}\xi + p^{*}_{59} \end{bmatrix}, \tag{32}$$

where the stress mode coefficients, p_{ij}^*, are presented in Appendix II.

Given the following constants arising from the regular structure of the strain modes

$$e_{1j} = b_2 z_1^j - b_1 z_2^j, \quad e_{4j} = a_1 z_2^j + a_2 z_1^j,$$

$$e_{2j} = b_3 z_1^j - b_1 z_3^j, \quad e_{5j} = a_1 z_3^j - a_3 z_1^j,$$

$$e_{3j} = b_2 z_3^j - b_3 z_2^j, \quad e_{6j} = a_3 z_2^j - z_2 z_3^j$$

where

j	z_1^j	z_2^j	z_3^j
1	−1	−1	1
2	1	−1	−1
3	1	1	1
4	−1	1	−1

(33)

and the general form for each stress mode given by

$$P_i^* = \begin{Bmatrix} p_{i1}\eta + p_{i2}\xi + p_{i3} \\ p_{i4}\eta + p_{i5}\xi + p_{i6} \\ p_{i7}\eta + p_{i8}\xi + p_{i9} \end{Bmatrix}, \tag{34}$$

the integration of eqn (26) yields explicit expressions for the components of the **G** matrix. The expressions are based on the most general form of orthonormalized stress modes in which most terms are zero for the simpler modes and the constants $(d_{ij})_k$ are elements of the **D** matrix computed at the kth evaluation point. In addition, for constant material properties, if all $(d_{ij})_k$ terms are discarded for $k > 1$, the resulting expressions reduce to an explicit form of the linear–elastic Pian–Sumihara element. The components g_{ij} with $i = 1, 2, 3, \ldots, 5$ and $j = 1, 2, 3, 4$ are given by

$$\begin{aligned} g_{i,2j-1} = (&p_{i1}^*\{(e_{1j}[(d_{11})_7 + 3(d_{11})_3] + e_{3j}[(d_{11})_4 \\ &+ 3(d_{11})_1 + 9(d_{11})_5/5] + (d_{11})_6 e_{2j}\} \\ &+ p_{i2}^*\{(e_{1j}[(d_{11})_8 + 3(d_{11})_2] + e_{2j}[(d_{11})_5 \\ &+ 3(d_{11})_1 + 9(d_{11})_4/5] + (d_{11})_6 e_{3j}\} \\ &+ p_{i3}^*\{(e_{2j}[(d_{11})_8 + 3(d_{11})_2] + e_{3j}[(d_{11})_7 \\ &+ 3(d_{11})_3] + 3e_{1j}[(d_{11})_5 + (d_{11})_4 + 3(d_{11})_1]\} \\ &+ p_{i4}^*\{(e_{1j}[(d_{12})_7 + 3(d_{12})_3] + e_{3j}[(d_{12})_4 \\ &+ 3(d_{12})_1 + 9(d_{12})_5/5] + e_{2j}(d_{12})_6\} \\ &+ p_{i5}^*\{(e_{1j}[(d_{12})_8 + 3(d_{12})_2] + e_{2j}[(d_{12})_5 \\ &+ 3(d_{12})_1 + 9(d_{12})_4/5] + e_{3j}(d_{12})_6\} \\ &+ p_{i6}^*\{(e_{3j}[(d_{12})_7 + 3(d_{12})_3] + e_{2j}[(d_{12})_8 \\ &+ 3(d_{12})_2] + 3e_{1j}[(d_{12})_5 + (d_{12})_4 + 3(d_{12})_1]\} \\ &+ p_{i7}^*\{(e_{4j}[(d_{33})_7 + 3(d_{33})_3] + e_{6j}[(d_{33})_4 \\ &+ 3(d_{33})_1 + 9(d_{33})_5/5] + e_{5j}(d_{33})_6\} \\ &+ p_{i8}^*\{(e_{4j}[(d_{33})_8 + 3(d_{33})_2] + e_{5j}[(d_{33})_5 \\ &+ 3(d_{33})_1 + 9(d_{33})_4/5] + e_{6j}(d_{33})_6\} \\ &+ p_{i9}^*\{(e_{5j}[(d_{33})_8 + 3(d_{33})_2] + e_{6j}[(d_{33})_7 \\ &+ 3(d_{33})_3] + 3e_{4j}[(d_{33})_5 \\ &+ (d_{33})_4 + 3(d_{33})_1]\})/9, \end{aligned}$$

$$\begin{aligned} g_{i,2j} = (&p_{i1}^*\{(e_{4j}[(d_{12})_7 + 3(d_{12})_3] + e_{6j}[(d_{12})_4 + 3(d_{12})_1 \\ &+ 9(d_{12})_5/5] + (d_{12})_6 e_{5j}\} \\ &+ p_{i2}^*\{(e_{4j}[(d_{12})_8 + 3(d_{12})_2] + e_{5j}[(d_{12})_5 \\ &+ 3(d_{12})_1 + 9(d_{12})_4/5] + (d_{12})_6 e_{6j}\} \\ &+ p_{i3}^*\{(e_{5j}[(d_{12})_8 + 3(d_{12})_2] + e_{6j}[(d_{12})_7 \\ &+ 3(d_{12})_3] + 3e_{4j}[(d_{12})_5 + (d_{12})_4 + 3(d_{12})_1]\} \\ &+ p_{i4}^*\{(e_{4j}[(d_{22})_7 + 3(d_{22})_3] + e_{6j}[(d_{22})_4 \\ &+ 3(d_{22})_1 + 9(d_{22})_5/5] + e_{5j}(d_{22})_6\} \\ &+ p_{i5}^*\{(e_{4j}[(d_{22})_8 + 3(d_{22})_2] + e_{5j}[(d_{22})_5 \\ &+ 3(d_{22})_1 + 9(d_{22})_4/5] + e_{6j}(d_{22})_6\} \\ &+ p_{i6}^*\{(e_{6j}[(d_{22})_7 + 3(d_{22})_3] + e_{5j}[(d_{22})_8 \\ &+ 3(d_{22})_2] + 3e_{4j}[(d_{22})_5 + (d_{22})_4 + 3(d_{22})_1]\} \\ &+ p_{i7}^*\{(e_{1j}[(d_{33})_7 + 3(d_{33})_3] + e_{3j}[(d_{33})_4 \end{aligned}$$

Table 1. Subroutine procedures

Name	Description	Name	Description
Mxmul	Matrix multiplication	Gmatrx	Explicit computation of **G** matrix
Mxadd	Matrix addition	Orthop	Computation of orthonormal stress modes
Invers	Matrix inversion	Spectrl	Spectral decomposition of **S** matrix
Statc	Static condensation	Main	Main program + minor subroutines

Table 2. Computational profiles of the nonlinear Pian–Sumihara (PS) element

PS-explicit				PS-numerical			
% time	Self (s)	Cumulative (s)	Procedure name	% time	Self (s)	Cumulative (s)	Procedure name
32.76	16.55	16.55	Spectrl	75.46	109.09	109.09	Mxmul
30.09	15.20	31.75	Mxmul	9.26	13.38	122.47	Mxadd
21.71	10.97	42.72	Gmatrx	6.50	9.39	131.86	Invers
3.17	1.60	44.32	Orthop	8.78	12.71	144.57	Main
12.27	6.20	50.52	Main				

$$+ 3(d_{33})_1 + 9(d_{33})_5/5] + e_{2j}(d_{33})_6\}$$

$$+ p_8^* \{(e_{1j}[(d_{33})_8 + 3(d_{33})_2] + e_{2j}[(d_{33})_5$$

$$+ 3(d_{33})_1 + 9(d_{33})_4/5] + e_{3j}(d_{33})_6\}$$

$$+ p_8^* \{(e_{2j}[(d_{33})_8 + 3(d_{33})_2] + e_{3j}[(d_{33})_7$$

$$+ 3(d_{33})_3] + 3e_{1j}[(d_{33})_5$$

$$+ (d_{33})_4 + 3(d_{33})_1]\})/9. \quad (35).$$

NUMERICAL STUDIES

Computer codes were generated to assess element computational characteristics. A description of the procedures used in the codes are presented in Table 1. The designation "main" combines the operations within the main program together with various minor subroutines which contribute insignificant computational cost. No optimization was attempted in terms of code preparation or CPU processing options such as vectorization or concurrency. The codes were run on a Hewlett Packard Apollo 400 series workstation in a Unix environment. The standard Unix profiler Gprof was used to characterize the time spent in performing various operations. Table 2 presents computational profiles and computer runtimes comparing the explicit and numerical generation of stiffness matrices in the nonlinear Pian–Sumihara quadrilateral element. An additional comparison is made to a four-node displacement-based element incorporating incompatible displacement modes which is presented in Table 3. The incompatible modes are based on quadratic functions and modified using a technique presented in Ref. [8] to identically satisfy the strong form of the patch test for incompatible elements. A 2nd-order Gaussian quadrature rule was used for all numerical evaluations in generating computational profiles. In generating the computational profiles, 10,000 element stifiness matrices were processed.

The computational profiles quantify the different characteristics of the explicit and numerical versions of nonlinear Pian–Sumihara element. In the explicit version, the eight spectral decompositions of the compliance matrix consume the greatest amount of computational cost (32.76%) while matrix multiplications constitute most of the computations in the numerical version (75.46%). The computational profile of the explicit version shows that the operations involved in forming the orthonormal stress modes is insignificant (3.17%) while the formation of the **G** matrix consumes 21.71% of the cost. The final evaluation of eqn (24), which is the only matrix operation performed in the explicit version, constitutes fully 30% of the cost in forming the element stiffness matrix. Comparing total cost, the explicit version requires only 34.95% of the processing time as the numerical evaluation and only 22.48% of the cost required in the incompatible displacement-based formulation. While this represents a significant reduction in processing cost, application of the developed methodology may be expected to show greater reductions in three-dimensional and higher-order hybrid element formulations. This issue is discussed in Remark II.

A second demonstration is made to show the accuracy of the nonuniform material representation in the explicit formulation. Because the basic computational characteristics have been shown above, a cantilevered beam under plane stress is solved where the material properties are not a function of the stress–strain state, but instead vary along the length of the beam. Such a problem is uncommon, but serves to illustrate the representation of material property variation in the clearest manner. The beam was analyzed using a coarse model of five elements. Two different mesh configurations were used as shown in Fig. 3; a uniform mesh was adopted to assess optimum element performance and a nonuniform mesh was used to assess distortion sensitivity to the simplifications currently incorporated in the explicit derivation. For simplicity, isotropic material properties were assumed with a linear variation of modulus as depicted in Fig. 4.

Table 3. Computational profile of incompatible displacement-based element

D-Based			
% time	Self (s)	Cumulative (s)	Procedure name
71.6	160.82	160.82	Mxmul
13.0	29.18	190.00	Mxadd
11.0	24.63	214.63	Statc
4.4	10.12	224.75	Main

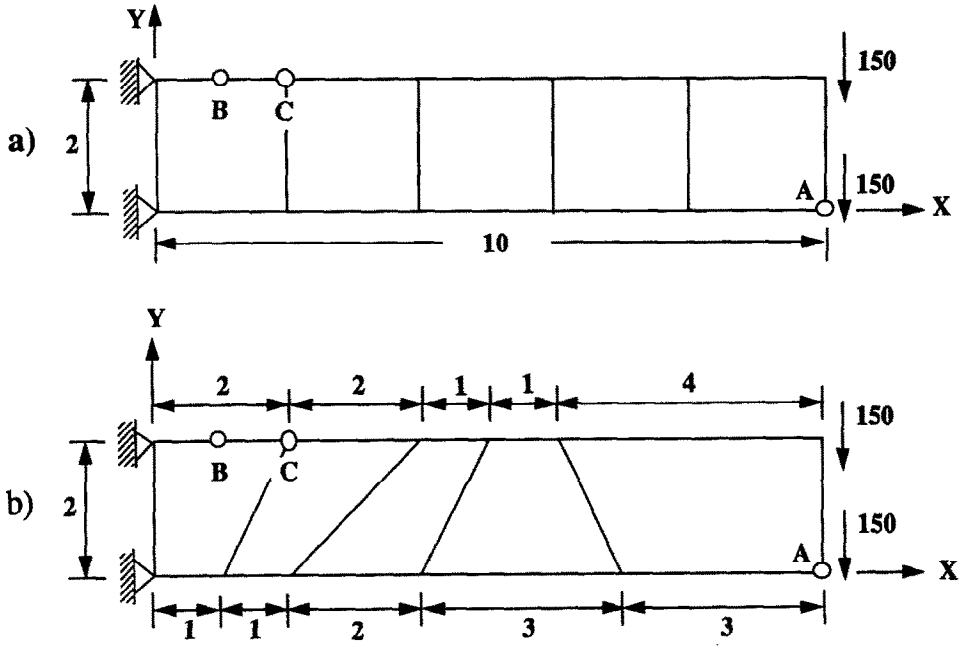

Fig. 3. Cantilevered beam configurations: (a) uniform mesh; (b) distorted mesh.

Table 4 depict solutions for the explicit and numerical hybrid element formulations together with results using an incompatible displacement-based element.

The above results show an excellent agreement between the explicit and numerical hybrid element formulations for both meshes; a small departure is seen in the tip deflection prediction in the explicit formulation using the irregular mesh due to the incorporated simplifications. The incompatible displacement-based element demonstrates good results for both stresses and displacements using a uniform mesh; however, in the distorted mesh, stress recovery is severely compromised. In general, the greater computational cost of the displacement-based element makes it unappealing.

REMARK 1

An important aspect of the above development involves the collocation error of the **D** matrix over the element domain using quadratic isoparametric shape functions. Because this matrix is computed as the square root of the material stiffness matrix, the individual components in **D** are interpolated to yield the approximate relation given above in eqn (15). A formal error estimate may be derived for arbitrary variation of material properties and order of collocation polynomials; however, a clearer illustration may be given by assuming a specific variation in the compliance matrix components as a function of a single coordinate, thus simplifying the error analysis to a one-dimensional demonstration. A linear function is selected in which a parameter, θ, is used to set the magnitude of variation in the material component denoted by C_0. The resulting square root distribution is given by

$$f(\xi) = C_0^{1/2}[1 + \theta(1 + \xi)]^{1/2}.$$

The values of $f(\xi)$ at the evaluation points along $\xi \in (-1, 1)$ are depicted in Fig. 5.

The quadratic isoparametric interpolation is given by

$$p(\xi) = C_0^{1/2}\{(1 + \theta)^{1/2} + \tfrac{1}{2}[(1 + 2\theta)^{1/2}]\xi + \tfrac{1}{2}[1 - 2(1 + \theta)^{1/2} + (1 + 2\theta)^{1/2}]\xi^2\}.$$

An error measure for point evaluation may be given by

$$E_p = \frac{|f(\xi) - p(\xi)|}{f(\xi)}.$$

A second error measure is associated with the difference between the integrated areas computed by the exact solution and the quadratic collocation. The integral of the exact distribution is given by

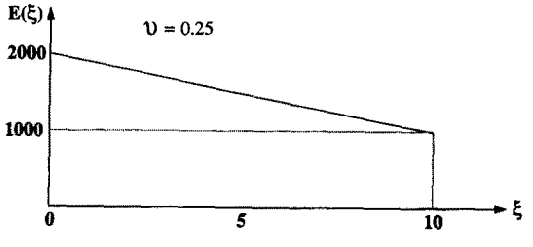

Fig. 4. Assumed linear variation in Young's modulus along beam length.

Table 4. Deflection of nonlinear cantilevered beam under end shear loading

(a) Uniform mesh				(b) Distorted mesh			
Elements	v_a	$\sigma_{x(b)}$	$\sigma_{x(c)}$	Elements	v_a	$\sigma_{x(b)}$	$\sigma_{x(c)}$
PS-explicit	−88.7	4045	3587	PS-explicit	−86.1	4048	3728
PS-numerical	−89.1	4050	3600	PS-numerical	−90.1	4047	3735
D-based	−89.0	4050	3586	D-based	−89.9	3276	3079
Exact	−90.4	4043	3601	Exact	−90.4	4043	3601

$$F(\xi) = \int_{-1}^{1} f(\xi)\,d\xi = \frac{2}{3\theta} C_0^{1/2}[(2\theta + 1)^{3/2} - 1],$$

while the integral of the collocated function is given by

$$P(\xi) = \int_{-1}^{1} p(\xi)\,d\xi$$

$$= \tfrac{1}{3} C_0^{1/2}[1 + 4(1 + \theta)^{1/2} + (1 + 2\theta)^{1/2}].$$

An error measure for the integral evaluation may be given by

$$E_i = \frac{|F(\xi) - P(\xi)|}{F(\xi)}.$$

Table 5 details error measures at the points of maximum expected error and the integrated error between the two assumed functions.

The above table indicates that the maximum point collocation error for a 40% variation in modulus ($\theta = 0.2$) over the segment is just over 1%. At $\theta = 0.5$, corresponding to a 100% variation in material properties, the point error increases to 11.2%. However, even when the properties vary by a factor of 3 ($\theta = 1.0$) over the segment, the integrated error, E_i, is still small, on the order of 4.05%.

REMARK II

With stresses assumed in natural coordinates, the procedure described herein may be applied directly. For higher-order elements, the approach of assuming tensorial stresses with a contravariant transformation using centroidal Jacobians to obtain Cartesian stresses is inaccurate and necessitates a formulation based on stresses assumed *a priori* in Cartesian coordinates. For assumed Cartesian stress fields, a fully explicit derivation may become overly cumbersome and computationally disadvantageous. In such cases the basic methodology is applied, but numerical quadrature of the scalar integrals arising in the weighted inner product and computation of **G**-matrix components is advocated. In higher-order elements, the reduction in computational cost afforded by adapting the present methodology is expected to be significantly greater than that demonstrated for the four-node quadrilateral element due to the larger order of the constituent matrices. The computational savings result from eliminating the cost of forming and inverting the complementary energy matrix, **H**, and by replacing the numerical quadrature of large-order matrix products by the quadrature of a small set of scalar integrals.

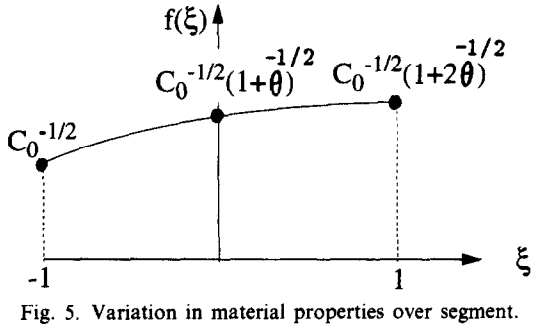

Fig. 5. Variation in material properties over segment.

CONCLUSION

The present effort has been aimed to enhance the computational efficiency of hybrid element formulations for nonlinear material analysis. The four-node Pian–Sumihara quadrilateral element was selected to illustrate methodology to derive explicit formulations accommodating nonconstant material properties. The derivation of an explicit element stiffness matrix has been shown to substantially reduce the computational cost in nonlinear analysis. The developed methodology is completely generic and may be applied to any hybrid element formulation to reduce the computational cost in linear and nonlinear applications. In the application to higher-order element formulations, an assumption of Cartesian stresses leads most efficiently to a combination of numerical evaluation of the scalar integrals involved in the orthonormalization process and in the integration of various integrals required in determining components of the **G** matrix. All other integrations may be performed analytically. The increase in efficiency demonstrated with a linear-order hybrid element is expected to be even more pronounced in higher-order element formulations due to the elimination of forming and inverting the complementary energy matrix and by replacing the

Table 5. Error measures for point and integral evaluation of material property interpolation

θ	$E_p(\xi = -\frac{1}{3})$	$E_p(\xi = \frac{1}{3})$	E_i
0.00	0.0	0.0	0.0
0.01	2.287×10^{-6}	2.262×10^{-6}	5.005×10^{-6}
0.05	2.603×10^{-4}	2.467×10^{-4}	2.683×10^{-6}
0.1	1.862×10^{-3}	1.681×10^{-3}	3.581×10^{-5}
0.2	1.211×10^{-2}	1.003×10^{-2}	4.109×10^{-4}
0.3	3.384×10^{-2}	2.606×10^{-2}	1.542×10^{-3}
0.4	6.739×10^{-2}	4.871×10^{-2}	3.710×10^{-3}
0.5	1.120×10^{-1}	7.658×10^{-2}	7.048×10^{-3}
0.6	1.664×10^{-1}	1.083×10^{-1}	1.158×10^{-2}
0.7	2.292×10^{-1}	1.429×10^{-1}	1.728×10^{-2}
0.8	2.993×10^{-1}	1.794×10^{-1}	2.406×10^{-1}
0.9	3.754×10^{-1}	2.171×10^{-1}	3.184×10^{-2}
1.0	4.565×10^{-1}	2.555×10^{-1}	4.051×10^{-2}

numerical quadrature of large-order matrix products with the analytical/numerical integration of a relatively small set of scalar integrals. The application of the above methodology can be expected to find general application in hybrid and mixed element formulations and provide a significant reduction in computational cost in generating element stiffness matrices for linear and nonlinear analysis.

REFERENCES

1. K. Y. Sze and C. L. Chow, Efficient hybrid/mixed elements using admissible matrix formulation. *Comput. Meth. appl. Mech. Engng* **99,** 1–26 (1992).
2. K. Y. Sze, Efficient formulation of robust hybrid elements using orthogonal stress/strain interpolants and admissible matrix formulation. *Int. J. numer. Meth. Engng* **35,** 1–20 (1992).
3. K. Y. Sze, A novel approach for devising higher-order hybrid elements. *Int. J. numer. Meth. Engng* **36,** 3303–3316 (1993).
4. E. Saether, Explicit determination of element stiffness matrices in the hybrid stress method. *Int. J. numer. Meth. Engng* **38,** 2547–2571 (1995).
5. E. Saether, Closed-form derivation of an 8-node hexahedral element stiffness matrix by the hybrid stress method *Commun. numer. Math. Engng* **11,** 775–787 (1995).
6. T. H. H. Pian and K. Sumihara, Rational approach for assumed stress finite element. *Int. J. numer. Meth. Engng* **20,** 1685–1695 (1984).
7. C. Lanczos, *Applied Analysis*. Dover, New York (1988).
8. C. C. Wu, M. G. Huang and T. H. H. Pian, Consistency condition and convergence criteria of incompatible elements: general formulation of incompatible functions and its application. *Comput. Struct.* **27,** 639–644 (1988).

APPENDIX I

Spectral decomposition

The spectral decomposition of an orthotropic material compliance matrix is given by

$$\mathbf{S}^{-1/2} = \mathbf{C}^{1/2} = \mathbf{Q}\Lambda^{1/2}\mathbf{Q}^{\mathrm{T}},$$

where the $\Lambda^{1/2}$ matrix is formed as a diagonal matrix of system eigenvalues given by

$$\Lambda^{1/2} = \mathrm{diag}[\varphi_1^{1/2}, \varphi_2^{1/2}, \varphi_3^{1/2}],$$

and the eigenvalues may be computed as

$$\varphi_1 = (-\sqrt{c_{22}^2 - 2c_{11}c_{22} + 4c_{12}^2 + c_{11}^2} + c_{22} + c_{11})/2,$$

$$\varphi_2 = (\sqrt{c_{22}^2 - 2c_{11}c_{22} + 4c_{12}^2 + c_{11}^2} + c_{22} + c_{11})/2,$$

$$\varphi_3 = c_{33},$$

in which c_{ij} are elements of the material stiffness matrix. The $\mathbf{Q}$ matrix is formed by the system eigenvectors as defined as

$$\mathbf{Q} = [\boldsymbol{\Phi}_1|\boldsymbol{\Phi}_2|\boldsymbol{\Phi}_3]$$

where the eigenvectors are given by

$$\bar{\boldsymbol{\Phi}}_1 = \begin{Bmatrix} c_{12} \\ \varphi_1 - c_{11} \\ 0 \end{Bmatrix}, \quad \bar{\boldsymbol{\Phi}}_2 = \begin{Bmatrix} \varphi_2 - c_{22} \\ c_{12} \\ 0 \end{Bmatrix}, \quad \bar{\boldsymbol{\Phi}}_3 = \begin{Bmatrix} 0 \\ 0 \\ c_{33} \end{Bmatrix},$$

and normalized as

$$N_i = (\bar{\boldsymbol{\Phi}}_i^{\mathrm{T}} \bar{\boldsymbol{\Phi}}_i)^{-1/2},$$

$$\boldsymbol{\Phi}_i = N_i \bar{\boldsymbol{\Phi}}_i.$$

APPENDIX II

Orthonormal stress mode components

The stress mode coefficients, p_{ij}^*, are given by

$$p_{13}^* = n_1, \quad p_{42}^* = n_4 c_{11}, \quad p_{43}^* = -n_4 c_{11}\lambda_2/\lambda_1,$$

$$p_{26}^* = n_1, \quad p_{45}^* = n_4 c_{21}, \quad p_{46}^* = -n_4 c_{21}\lambda_2/\lambda_1,$$

$$p_{39}^* = n_1, \quad p_{48}^* = n_4 c_{31}, \quad p_{49}^* = -n_4 c_{31}\lambda_2/\lambda_1,$$

$$p_{51}^* = n_5 c_{12}, \quad p_{52}^* = -n_5 c_{11}\phi, \quad p_{53}^* = -n_5\theta_1,$$

$$p_{54}^* = n_5 c_{22}, \quad p_{55}^* = -n_5 c_{21}\phi, \quad p_{56}^* = -n_5\theta_2,$$

$$p_{57}^* = n_5 c_{32}, \quad p_{58}^* = -n_5 c_{31}\phi, \quad p_{59}^* = -n_5\theta_3,$$

in which

$$\phi = -n_4^2(c_{12}c_{11} + c_{22}c_{21} + c_{32}c_{31})\lambda_2\lambda_3/\lambda_1,$$

$$\theta_1 = (c_{12}\lambda_3 + \phi c_{11}\lambda_2)/\lambda_1,$$

$$\theta_2 = (c_{22}\lambda_3 + \phi c_{21}\lambda_2)/\lambda_1,$$

$$\theta_3 = (c_{32}\lambda_3 + \phi c_{31}\lambda_2)/\lambda_1,$$

and normalizing factors are given by

$$n_1 = \lambda_1^{-1/2},$$

$$n_4 = [(c_{11}^2 + c_{21}^2 + c_{31}^2)(\lambda_5 - \lambda_2^2/\lambda_1)]^{-1/2},$$

$$n_5 = \left[\sum_{i=1}^{3}(c_{i2}^2 - 2c_{i2}\theta_i\lambda_3 + \phi^2 c_{i1}^2\lambda_5 + 2\phi c_{i1}\theta_i\lambda_2 + \theta_i^2\lambda_1)\right]^{-1/2}.$$

The determinant of the Jacobian for two-dimensional transformations is given by

$$|\mathbf{J}| = J_0 + J_1\xi + J_2\eta,$$

where

$$J_0 = a_1b_2 - a_2b_1, \quad J_1 = a_1b_3 - a_3b_1, \quad J_2 = a_3b_2 - a_2b_3.$$

The scalar integrals arising in the inner product to evaluate to

$$\lambda_1 = \int_{-1}^{1}\int_{-1}^{1} |\mathbf{J}|\, d\xi\, d\eta = 4J_0,$$

$$\lambda_2 = \int_{-1}^{1}\int_{-1}^{1} |\mathbf{J}|\xi\, d\xi\, d\eta = 4J_1/3,$$

$$\lambda_3 = \int_{-1}^{1}\int_{-1}^{1} |\mathbf{J}|\eta\, d\xi\, d\eta = 4J_2/3,$$

$$\lambda_4 = \int_{-1}^{1}\int_{-1}^{1} [|\mathbf{J}|\xi\eta\, d\xi\, d\eta = 0,$$

$$\lambda_5 = \int_{-1}^{1}\int_{-1}^{1} [|\mathbf{J}|\xi^2\, d\xi\, d\eta = 4J_0/3,$$

$$\lambda_6 = \int_{-1}^{1}\int_{-1}^{1} [|\mathbf{J}|\eta^2\, d\xi\, d\eta = 4J_0/3.$$